Physical modelling of wave propagation and wave breaking in a wave channel

Diogo R.C.B. Neves[1], Luiz A. M. Endres[2], Conceição J.E.M. Fortes[3] and Takashi Okamoto[4]

Abstract

The presented work describes a wide range of wave channel tests performed at the National Laboratory of Civil Engineering (LNEC), considering different incident wave conditions, with the objective of studying the wave breaking hydrodynamics. Special attention was made to the end of the wave breaking process. The experimental setup, the incident wave conditions, the equipment and the performed measurements (free surface elevation and particle velocity) are herein described. Time, spectral and statistical analysis based upon the measured data are also performed and presented. Moreover, a more deepen analysis related: (i) the relative wave height (H/d); (ii) the wave celerity; (iii) the two-dimensional distribution of the particle velocities components in the xy, xz and yz planes and; (iv) the average wave direction and spreading angle is carried out and presented. Vertical velocity profiles are also presented.

Keywords: wave breaking, wave propagation, physical modelling, wave channel

1 Introduction

The determination of the wave breaking zone is an important matter for studies referring coastal hydrodynamics and sediment transport. More accurately, the location and extension of the wave breaking section are two of the main factors for the coastal structures foundation and stability or for the nearshore sediment dynamics.

Many studies aimed to analyze the initial process of the wave breaking (Goda, 1970; Weggel, 1972; Tsai et al., 2004; Camenen and Larson, 2007) however the processes after the initial point until the end of the wave breaking are still object of a broad discussion in the scientific community (Svendsen et al., 1978 and 2003; Tsai et al., 2004). The traditional wave breaking indexes are usually related with the initial location of the wave breaking, leaving in background the end section of the process, which is, as mentioned above, especially important in coastal dynamics studies and for the set up of maritime structures.

Following this reasoning, an extensive set of experimental tests was carried out to study the wave breaking characteristics and hydrodynamics, considering different incident conditions. Special attention is given to data from the wave breaking section and especially at the end of it. The experimental tests were performed in a wave channel with a 32.4 m length, at the National Laboratory of Civil Engineering (LNEC), Lisbon, Portugal. The bottom profile of the wave channel consisted essentially in different bottom slopes. The tested wave conditions represented a combination of regular waves with wave periods of 1.1, 1.5, 2.0 and 2.5 s and wave heights of 12, 14, 16 and 18 cm.

This paper presents the experimental conditions, the incident wave conditions and the experimental procedures (section 2). Data and results from time, spectral and statistical analysis are presented (section 3). Moreover, a more in-depth data analysis was carried out for the calculation of several parameters, such as: (i) the definition of the wave breaking zone; (ii) the relative wave height (H/d); (iii) the wave celerity; (iv) the two-dimensional distributions of the

[1] National Laboratory of Civil Engineering, Av. do Brasil 101, Lisbon, 1700-066, Portugal, dneves@lnec.pt

[2] Universidade Federal do Rio Grande do Sul, Av. Bento Gonçalves 9500, Porto Alegre, 91501-970, Brazil, endres@ufrgs.br

[3] National Laboratory of Civil Engineering, Av. do Brasil 101, Lisbon, 1700-066, Portugal, jfortes@lnec.pt

[4] Hiroshima University, 1-5-1 Kagamiyama, Higashi-Hiroshima, Hiroshima, 739-8529, Japan, tokamoto@hiroshima-u.ac.jp

velocity components in the xy, xz and yz planes; (v) and the directional analysis with the evaluation of the spreading angle. Vertical velocity profiles are also presented. Finally, the conclusions are drawn in section 4.

2 Experimental Settings

Wave tank experiments were conducted at the National Laboratory of Civil Engineering (LNEC) in Lisbon, Portugal. The wave flume is 32.4 m long from the wave maker (Figure 2(a)). A beach profile, with different bottom slopes, was constructed as shown in Figure 1. The slope angle of the front face of the bar and the beach section was fixed with 1:20 and the slope of the lee side of the bar was of 1:80. Water depth was measured to be 10 cm at the crest of the 1:20 bar.

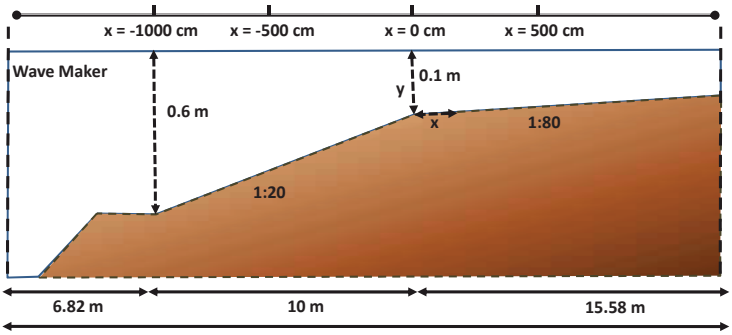

Figure 1: Wave Channel profile and positions along the longitudinal (x) axis

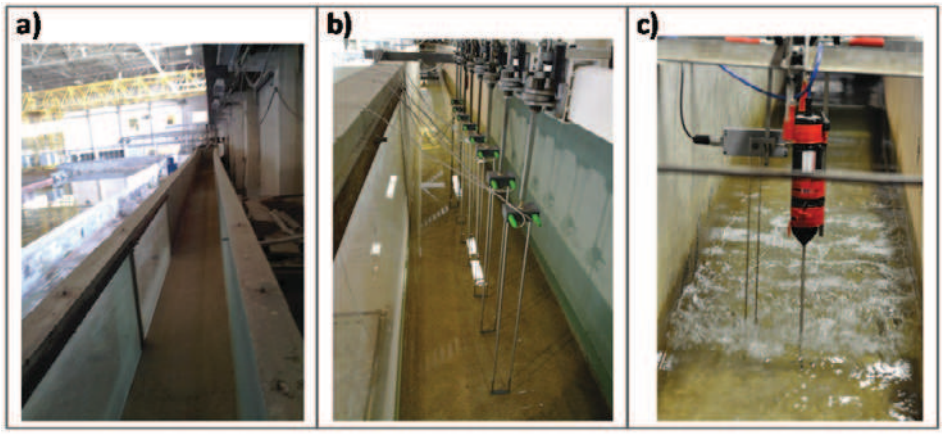

Figure 2: (a) Wave Channel; (b) the 8 gauge mobile structure; (c) The ADV and the resistive gauge

2.1 Incident wave characteristics and experimental tests

A piston-type wave maker generated a combination of regular waves with four wave periods (T=1.1, 1.5, 2.0 and 2.5 sec) and four wave heights (H=12, 14, 16, and 18 cm). The case of T=1.1 sec, and H=18 cm presented a very steep wave that broke in front of the wave maker, therefore, this incident wave condition was excluded from the experimental tests. Thus, in total, for each position along the canal, fifteen combinations of waves were tested.

The total set of experiments was divided in three phases: (i) Phase I - Free surface elevations measurements along the channel with an 8 gauge mobile structure; (ii) Phase II - Particle velocity measurements along the channel in the middle of the water column, using an Acoustic Doppler Velocimeter (ADV) sensor; (iii) Phase III - Vertical velocity profiles using the same ADV sensor. In phases II and III, together with the particle velocity measurements, free surface elevations were measured simultaneously in the same transverse section of the channel.

2.2 Equipment and experimental procedures

At Phase I, free surface elevations were measured using an eight gauge mobile structure, Figure 2(b). This structure moved along the channel, and measurements were taken from the beginning of the first ramp (x = -1000 cm) till x = 560 cm when the wave breaking is showed to be completely over for every incident wave condition. In order to calibrate the input wave height, a wave gauge was installed at the toe of the front face of the first slope (x = -1080 cm). Each gauge in the mobile structure was separated by a fixed distance (20 cm), and measurements separated by 10 cm were taken along the covered area.

For Phases II and III, the particle velocity was measured by an ADV with a down-looking probe, enabling the three orthogonal components of the suspended particle velocities (volume measurements), Figure 2(c). Together with the ADV, a resistive gauge was placed for simultaneous measurements of the free surface elevation (Figure 2(c)). In Phase II, the ADV probe was located in the middle of the water column. Measurements were obtained between x = -200 cm and x = 560 cm, at every 10 cm, while between x = -1000 cm and x = -200 cm the interval was of 100 cm.

For the phase III, vertical velocity profiles were measured (separated by 5 cm in the vertical axis (z)) for selected (x) locations (x = -1000; -500; -100; 0; 50; and 150 cm).

The sampling frequency of all the measurements was of 25 Hz and each experimental test (incident wave) had the duration of 490 s.

The wave breaking section (from the beginning till the end of the wave breaking zone) was defined by visual observation. The beginning and the end of the wave breaking zone was considered when the air bubbles started tipping over the crest and vanished from the water, respectively. Considering the nature of these observations, about 50 samples were collected and an average value was determined.

3 Results

For each of the 15 incident wave conditions, time series of the free surface elevation and the particle velocity along the wave channel (and especially from x = -1000 cm to x = 560 cm) were obtained. Based on the data, different types of data analysis were considered:

Phase I – Time, spectral, and statistical analysis of the free surface elevation measurements. Also, the wave celerity and the relative wave height (H/d) along the wave channel were calculated for each wave condition.

Phase II – Time, spectral, and statistical analysis of the particle velocity measurements. Moreover, the ADV measurements allowed the calculation of the particle velocities main characteristics, the two-dimensional distributions of velocity components at the (xy), (xz) and (yz) planes and the average wave direction as well as the directional dispersion (spreading).

Phase III – Time analysis of the vertical velocity profiles in the selected locations of the wave channel.

In the next sections, beyond the beginning and ending of the wave breaking zone, for each phase, some samples are presented from the calculated results. The incident wave condition of T = 1.5 s and H = 18 cm was chosen as an example of results for the majority of the presented samples.

3.1 Wave breaking zone

As referred in section 2, the wave breaking section was defined for each one of the 15 incident waves. About 50 samples were obtained and an average value was determined for the initial and terminal location of the wave breaking. Both locations were defined by eye observation (Table 1).

Table 1: Initial and terminal location of the wave breaking section

	Initial location of the wave breaking section				Terminal location of the wave breaking section			
T (s) / H(cm)	1.1	1.5	2.0	2.5	1.1	1.5	2.0	2.5
12	-267	-212	-203	-220	205	265	330	445
14	-332	-276	-289	-270	200	245	330	445
16	-427	-340	-361	-295	200	245	305	428
18		-395	-410	-367		245	293	415

3.2 Phase I results

3.2.1 Relative Wave Height

The relative wave height (H/d) is often used as an index for the wave breaking section in shallow water conditions. Dally et al. (1985) considers this index as reference for a stabilized wave condition.

Figure 3 shows, for all the 15 incident wave conditions, the relative wave height evolution from the top of the bar until the end of the surf section. The x-axis was normalized by the wave breaking section, x = 0 indicates the beginning and x = 1 the terminal location of wave breaking (see 3.1). From the figure it can be concluded that the curve of H/d has two phases. Before the wave breaking zone the curve is steeper, increasing rapidly, while after the wave breaking the slope presents a smoother curve. Between x = 0.0 and 0.6, H/d decreases until H/d = 0.35 ≈ 0.65 depending on the incident wave condition, this value remains constant until x = 1. The average rate of H/d at the end of the wave breaking section is of 0.45, for an incident wave of T = 1.5 s and H = 18 cm (see the “Poly. (T=15s & H=18 cm)” that represents the trendline for the T = 1.5 s and H = 18 cm incident wave condition).

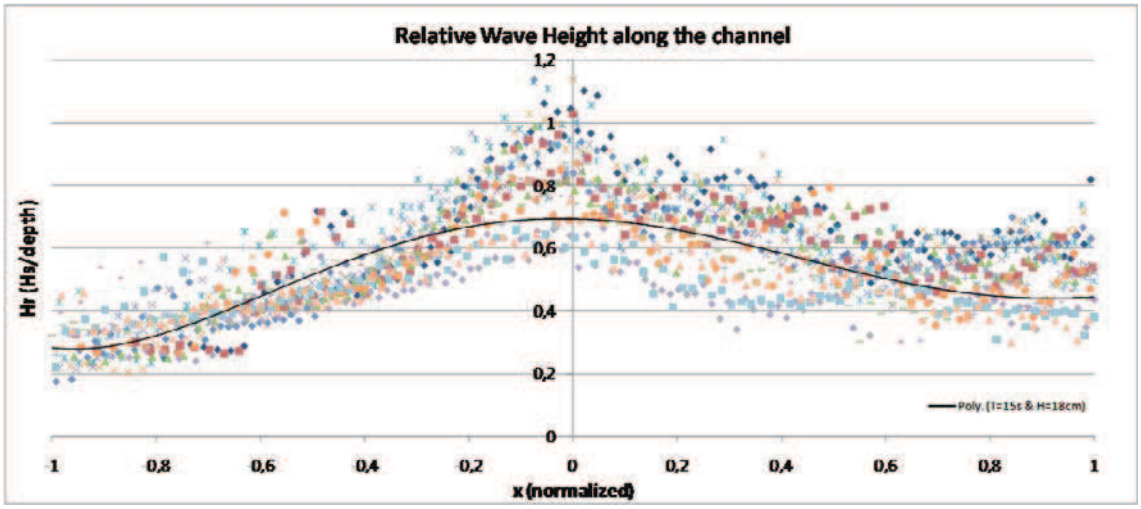

Figure 3: Relative wave height evolution (x = 0 is the beginning and x = 1 is the end of the wave breaking) using a normalized scale for all the wave conditions.

3.2.2 Wave Celerity

To calculate the wave celerity it is necessary to estimate the average time required for the passing waves between each two consecutive gauges. The wave passing time was calculated

as the one corresponding to the largest cross-correlation value between the full records of each pair of gauges. This method was applied by Okamoto et al. 2010.

Figure 3 shows the wave celerity along the channel for the incident wave conditions of H = 18 cm, and wave periods of T = 1.5, 2.0 and 2.5 s. In the figure, the “theoretical curve” is the curve of the values of $\sqrt{g\,h}$ and the fit curves “Poly. (H(18cm)T15(s))", "Poly (H(18cm)T20(s))" and "Poly (H(18cm)T25(s))" correspond to the "H(18cm)T15(s)", "H(18cm)T20(s)" and "H(18cm)T25(s)" incident wave conditions.

For the three periods: (i) at the initial section there is a slightly increase of the celerity; (ii) then, the wave celerity is almost constant; (iii) after x = -400 cm, where the wave breaking occurs, the celerity decreases, following the depth reduction of the channel, starting first in the minor periods. This behavior agrees with the occurrence of earlier wave breaking for shorter periods (see 3.1); (iv) in the final section of the channel the large reduction of the slope and the end of the wave breaking section motivates the curve smoothing and the tendency to collapse in one curve.

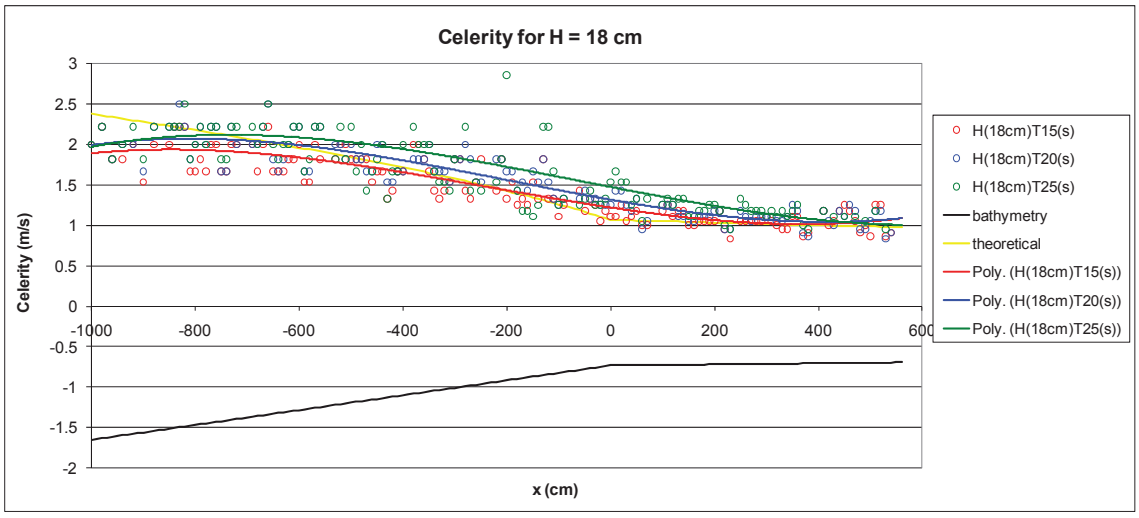

Figure 3: Wave celerity results along the channel for incident waves of H = 18 cm and T = 1.5, 2.0 and 2.5 s.

3.3 Phase II results

3.3.1 Time, spectral, and statistical analysis of the velocity data

The statistical analysis consisted in determining the average, standard deviation, skewness (distortion) and kurtosis of the particle velocity values (V_x) recorded for each incident wave condition along the x-axis position (positive V_x values are toward the wave maker) (Sancho et al., 2001), Figure 4. The average of the velocity values at each record was calculated through the average of all measured values in the record. The averages of the maximum and minimum velocities were calculated by the identification of each "wave" using the criterion of the downward zero crossing, each intersection was considered effective when there were at least two points before and after the zero reference.

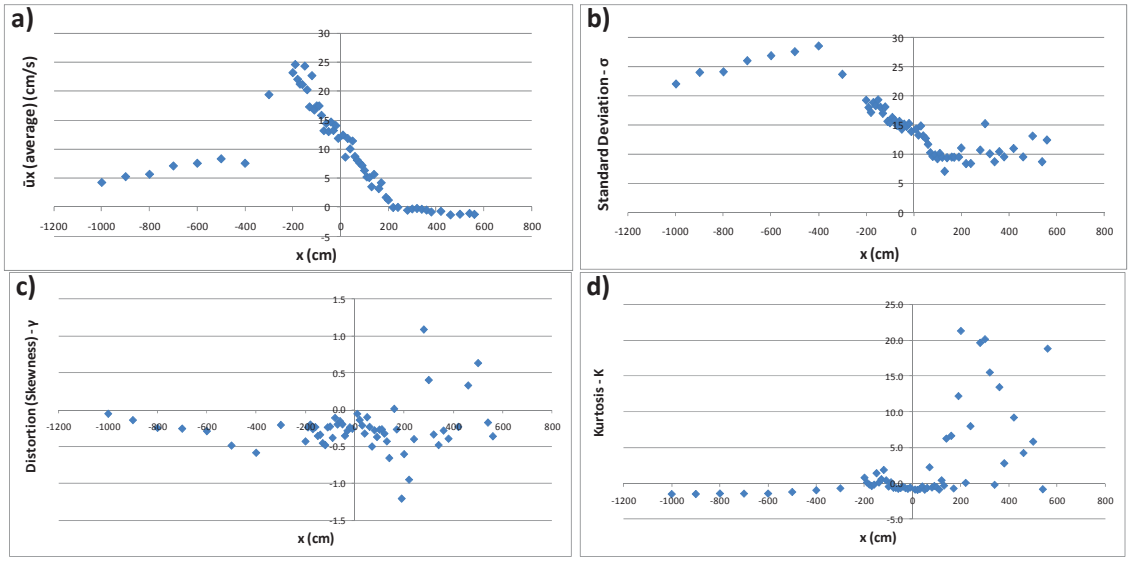

Figure 4: (a) Average, (b) the standard deviation, (c) skewness and (d) kurtosis of the velocity (Vx) values along the channel, for T = 1.5 s and H = 18 cm

Figure 4(a) shows that after the breaking point (near x = -400 cm), the average values increase abruptly and when the wave collapses (around x = -200 cm) those values start to decrease till they become almost constant by the end of the wave breaking, after x = 200 cm. The standard deviation (Figure 4(b)) depicts values that are similar to the average of the velocities, first an increment till the breaking point followed by a decrease till the end of the surf section, after that, some scattered values show some inconsistency probably due to the harmonics generation created by the bottom slope or by the wave breaking effect. For the skewness and the kurtosis (Figure 4(c)(d)), a general trend can be observed indicating huge differences at the end of the wave breaking (after x = 100 cm) possibly due to the appearance of some waves generated by the bottom slope and by the wave breaking effect.

3.3.2 Two-dimensional distribution of the three orthogonal components of the velocity

In this section the analysis of the two-dimensional distributions of the velocity components in the xy, xz and yz planes is performed. The procedure followed, firstly, the evaluation of the parameters (E_x, E_y, E_z, Figure 5). E_x, E_y and E_z are the differences between the averages of the positive and negative velocities for each orthogonal component (x, y, z) measured by the ADV. In Figure 6, the E_z/E_x, E_y/E_x and E_y/E_z ratios are represented for an incident wave condition of T= 1.5 s and H = 18 cm.

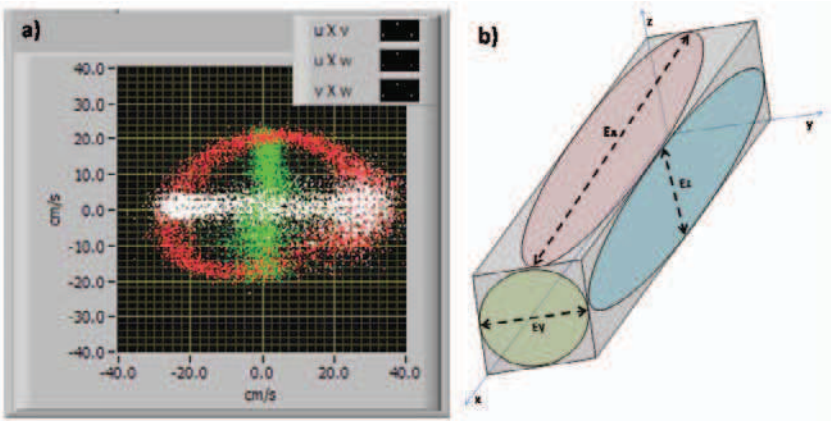

Figure 5: Typical two-dimensional distributions of the velocity components (a) the recorded data cloud (u = Vx, v = Vy, w = Vz) and (b) parameters lengths schematically represented

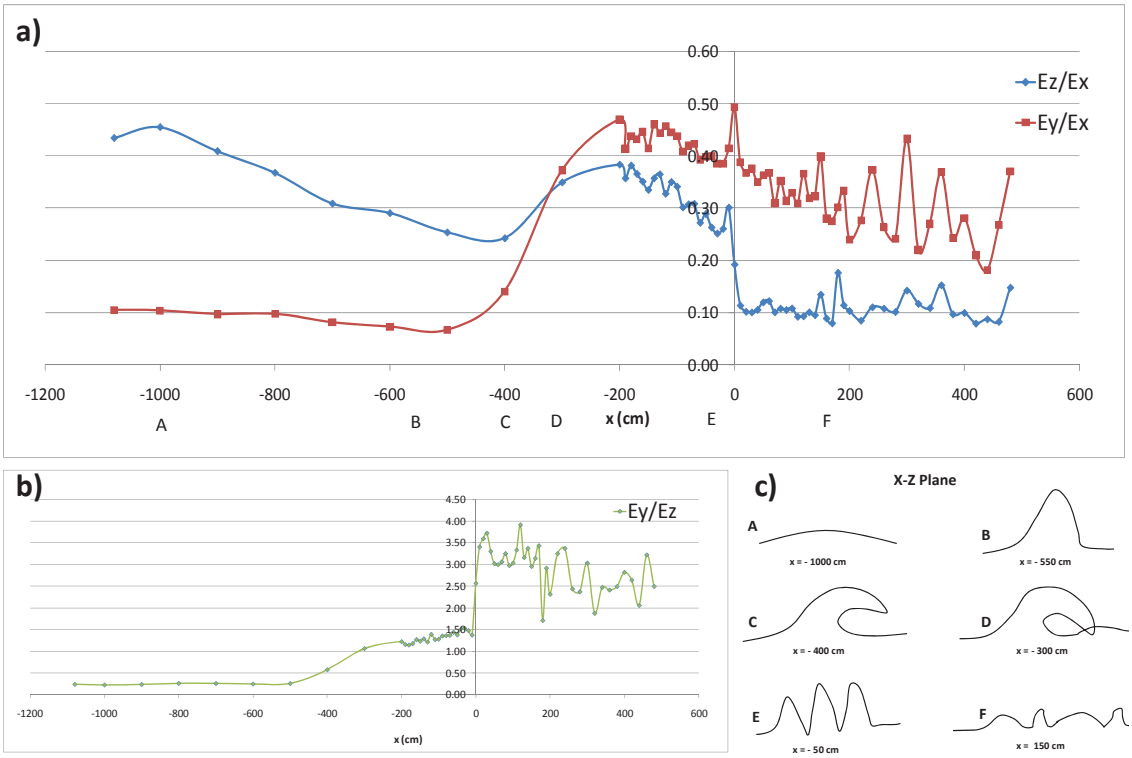

Figure 6: (a) Ez/Ex and Ey/Ex; (b) Ey/Ez ratios along the x axis of the channel T = 1.5 s and H = 18 cm; (c) wave shape in the xz plane for positions along the channel (A-F)

From Figure 6, one can conclude that the beginning of the channel and approaching the wave breaking zone, the ratios are $E_y/E_x<0.1$ and $E_y/E_z<0.4$, not far from the ideal, $E_y/E_x = E_y/E_z = 0$.

Later, though with an increase in the ratios values involving the parameter E_y, the results remain fairly unchanged until the position near x = - 500 cm, when a new change is felt, particularly considering the ratio E_y/E_z.

The position $x \cong$ - 400 cm represents the beginning of the wave breaking section, from this point an abrupt increase of the E_z/E_x ratio occurs till x = -200 cm. For x > -200 cm, the values decrease, forcing a stretch of the waveform in the longitudinal direction of the channel.

Interesting is to observe that the wave breaking affects differently the three ratios (E_z/E_x; E_y/E_x; E_y/E_z). Following E_z/E_x the response to the wave breaking is felt 100 cm later than both E_y/E_x and E_y/E_z. Around x = -400 cm the E_z/E_x starts to increase, meanwhile the curves of the ratios E_y/E_x and E_y/E_z had already begun to increase around x = -500 cm. Figure 6 shows clearly the transformation of the E_x component into the E_z and E_y components. This is mainly due to the rolling effect of the wave that obliges the water spreading during the wave breaking phenomena. The transverse component (E_y) is due to the turbulent mixture from the roller effect of the breaking wave, which starts around x = -500 cm.

3.3.3 Average wave direction and dispersion

One highlight of this work was the directional analysis (based on the simultaneous measurements of the particle velocities and the free surface values), that at first approach would not make sense in a 2D wave channel. Nevertheless, due to the generated turbulence in the wave breaking process, the directional spreading is observed along the wave propagation on the wave channel. Thus, the directional analysis of the experimental data may constitute a framework for the turbulence quantification associated with the wave breaking phenomena.

To obtain the directional wave spectrum the method developed by Longuet-Higgins (Dean & Dalrymple, 1993) can be used. This method, in addition to the free surface elevation records, considers also the simultaneous records of the velocities in the horizontal plane distribution. In this method, the directional spectrum is expressed by a Fourier series. According to Trageser

and Elwany (1990), the estimation of the mean wave direction as a function of frequency $\theta(f)$ is accurate. However, the estimation of the directional dispersion value can be coarse for a limited number of coefficients.

The average wave direction and dispersion were calculated by using the simultaneous measurements of the particle velocity and the free surface elevation made along the x axis of the channel. The obtained results for the spreading angle and wave direction are shown through the Figure 7 below.

According to Figure 7, the main direction angles remain around the original generation value (270°). The breaking wave still propagates into the same direction and keeps the wave train unchanged. However, the growth of the spreading angle during the wave breaking process is remarkable. In fact this analysis presents very low spreading values before the wave breaking, increasing during the wave breaking, specially just before x = 0, in order to decrease considerably after the end of the wave breaking section. This might also indicate that after the wave breaking, the residual frequency changes into more waves with different frequencies that propagate independently (Okamoto *et al.*, 2010).

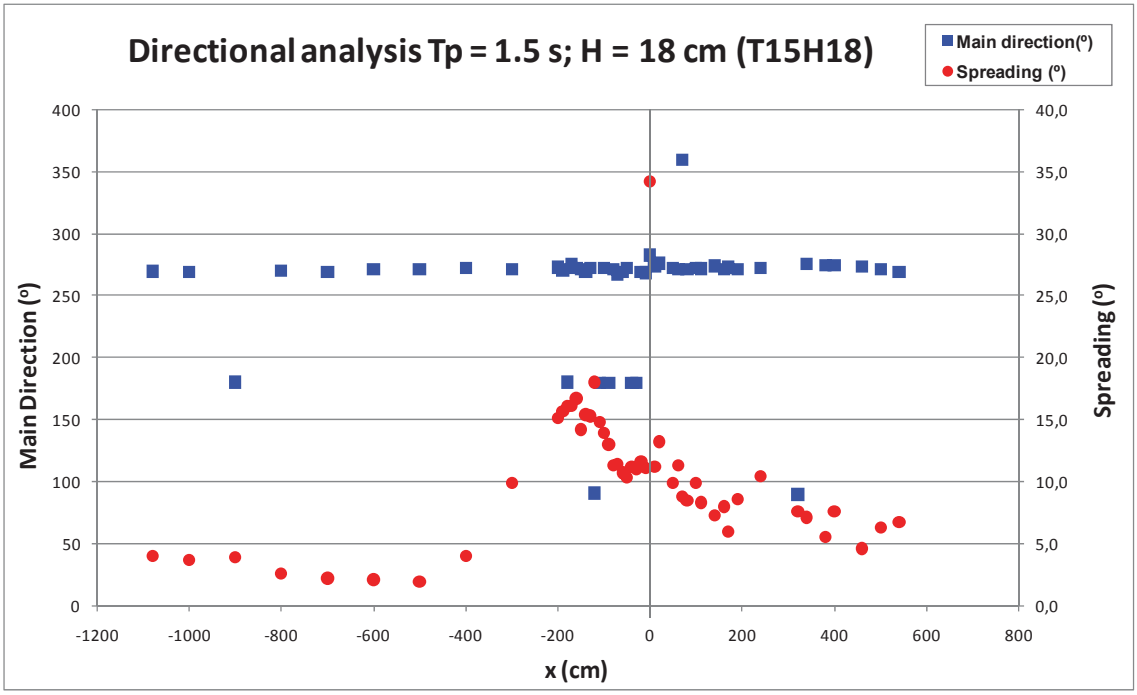

Figure 7: Main direction (º) and spreading angle for T = 1.5 s and H = 18 cm

3.4 Phase III - results

3.4.1 Vertical Velocity profiles

To analyse the vertical profiles of the velocity, the maximum, minimum and average values of the velocities were calculated (V_x) (Figure 8). The maximum, minimum and average values represent, respectively, the maximum, minimum and average of the complete record. It is important to note that the positive values of the velocities are towards the paddle, in the opposite direction of the wave propagation.

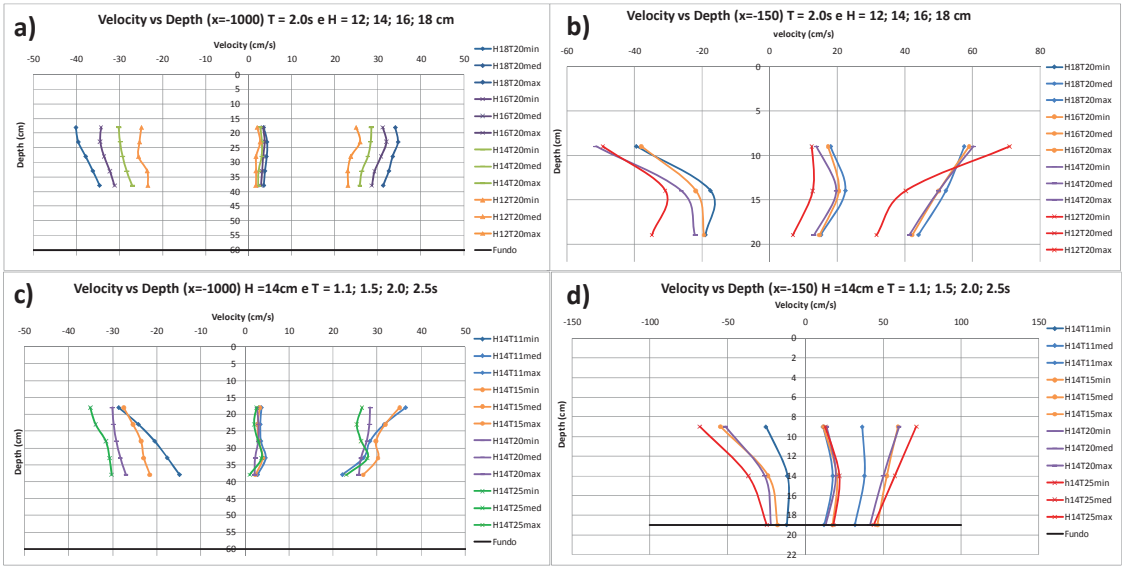

Figure 8: Vertical velocity profiles in (a) x = -1000 cm and (b) x = -150 cm for T = 2.0 s and H = 12, 14, 16 and 18 cm; (c) x = -1000 cm and (d) x = -150 cm for a incident wave of H = 14 cm and T = 1.1, 1.5, 2.0 and 2.5 s

Figure 8 shows that the greater velocities happen to be in occasions of bigger wave heights and periods. For x = -1000 cm, the values do not vary significantly along the vertical axis (about 5 cm/s). For the position x = -150 cm (Figure 8(b)(d)), the bottom effect produces a 20 cm/s velocity differences for the maximum and minimum values.

4 Conclusions

In this paper, recent physical modelling tests on a wave channel from the National Laboratory of Civil Engineering (LNEC) in Lisbon were presented. The tests aimed to study the wave breaking hydrodynamics on a beach profile with variable bottom slopes since its beginning till the very end.

The physical modelling was performed on a wave channel, built for the regular wave propagation studies, with a bottom characterized by a flat section followed by two ramps with 1:20 and 1:80 slopes respectively, forming a characteristic beach profile. The tested waves resulted from a combination of 1.1, 1.5, 2.0 and 2.5 s periods with wave heights of 12, 14, 16 and 18 cm. The measured data from the resistive gauges (free surface) and the Acoustic Doppler Velocimeter (ADV) enabled the calculation of several parameters, such as the wave celerity, the relative wave heights, the two-dimensional distributions of the velocity components in the xy, xz and yz planes, the main wave direction and the spreading angle of the wave propagation, the initial and final location of the wave breaking section was observed and the temporal analysis of the vertical velocity profiles in selected locations of the wave channel are presented.

From the tests with the physical model, a wide set of wave data (free surface elevation and particle velocity) along the channel and especially in the wave breaking section is available. This constitutes an important output of this work since it can be used to understand more deeply the wave breaking process but also for the establishment/improvement of the wave breaking numerical models and its validation.

5 Acknowledgements

This study is funded by the FCT under the contracts of SFRH/BPD/20508/2004, PTDC/ECM/73145/2006 and PTDC/ECM/67411/2006 and FCT/CAPES (Brazil) – “Building a Base for Research and Knowledge in Coastal Engineering”.

6 References

Camenen, B., M. Larson (2007). Predictive Formulas for Breaker Depth Index and Breaker Type. Journal of Coastal Research: Volume 23, Issue 4: pp. 1028 – 1041, West Palm Beach (Florida), ISSN 0749-0208.

Dally, W. R., R. G. Dean, R. A. Dalrymple (1985). Wave height variation across beaches of arbitrary profile. Journal of Geophvsical Research, Vol. 90, No. C6, Nov. 20, 11917-11927.

Dean, R. G., R. A. Dalrymple (1993). Water Wave Mechanics for Engineers and Scientists. World Scientific, Singapore.

Goda, Y. (1970). A Synthesis of Breaking Indices. Transactions of JSCE, Vol.2, Part 2, 39-49.

Okamoto, T., C. J. Fortes, D.R. Basco (2010). Bore propagation speed at the termination of wave breaking. ICCE, Proceedings of 32nd Conference on Coastal Engineering, Shanghai, China.

Sancho, F., P.A. Mendes, J.A. Carmo, M.G. Neves, G.R. Tomasicchio, R. Archetti, L. Damiani, M. Mossa, A. Rinaldi, X. Gironella, A.S. Arcilla (2001) Wave hydrodynamics over a barred beach. Proc. Int. Symp. on Ocean Wave Measurement and Analysis, “Waves 2001”, S. Francisco, ASCE.

Svendsen, I.A., P.A. Madsen, J.B. Hansen (1978). Wave characteristics in the surf zone. Proc. of 16th ICCE, ASCE, 520-539

Svendsen, I.A., W. Qin, B.A. Ebersole (2003). Modelling waves and currents at the LSTF and other laboratory facilities. Coastal Engineering, 50, Issues 1-2, 19-45, ISSN 0378-3839, DOI: 10.1016/S0378-3839(03)00077-2

Trageser, J.H., H. Elwany (1990). The S4DW, an integrated solution to directional wave measurements. Proc. IEEE Working Conf. on Current Measurement, 154-168, DOI: 10.1109/CURM.1990.110902

Tsai C.P., H. B. Chenb, H. H. Hwungc, M. J. Huang (2004). Examination of empirical formulas for wave shoaling and breaking on steep slopes. Ocean Engineering, Volume 32, Issues 3-4, Pages 469-483, ISSN 0029-8018, DOI: 10.1016/j.oceaneng.2004.05.010

Weggel, J. R. (1972). Maximum Breaker Height. Journal of Waterways, Harbors, and Coastal Engineering Division, ASCE, vol. 98,529-54